

High-bandwidth tip-tilt compensation for small telescope systems

Andreas Sinn, Christian Schwaer, Peter Kremsner, and Georg Schitter

Automation and Control Institute (ACIN), TU Wien, Gusshausstrasse 27-29, 1040 Vienna, Austria

ABSTRACT

This publication presents a high-bandwidth tip-tilt compensation system for small telescopes. It is designed with respect to the requirements of applications such as free-space optical (FSO) communication and space debris imaging, where high tracking speeds up to several degrees per second are required and lead to an increased disturbance bandwidth. A quad-photo-diode (QPD) is used to measure the tip-tilt errors and compensate them in a closed-loop manner by a fast-steering mirror (FSM). Feedback controllers are designed based on a measured disturbance spectrum. Measurement results obtained from reflected sunlight of a low-Earth-orbit (LEO) object successfully demonstrate the potential of the proposed compensation system, effectively reducing the RMS tip-tilt error by up to a factor of 5.

Keywords: tip-tilt compensation, fast steering mirror, small telescope system, optical communication

1. INTRODUCTION

Small optical telescope systems with a diameter of up to 1 m are a flexible and affordable option for many applications in space research. This includes classical astronomy,¹ observation networks,^{2,3} space debris imaging,⁴⁻⁶ satellite laser ranging (SLR)^{7,8} as well as free-space optical satellite communication.⁹⁻¹²

The achievable performance of all of those applications, which typically use visible or near infrared wavelength ranges, is degraded by atmospheric turbulence,^{13,14} wind-shake and vibrations,¹⁵ as well as pointing and tracking imperfections.¹⁶ One possible approach to tackle this problem is tip-tilt compensation of disturbances acting onto the optical channel and the telescope system.¹⁷ These disturbances are measured and corrected, typically in a closed-loop manner using a low-order wavefront sensor such as a QPD and a FSM. Although this approach is well established as part of adaptive optical systems,^{13,18-20} applications such as FSO satellite communication and space debris imaging, where (typically LEO) objects are tracked at rates up to several degrees per second, introduce new challenges.²¹ Due to the fast relative motion of the field of view of the telescope through the atmosphere, the resulting relative velocity may add on top of the already present winds, shifting the temporal disturbance spectrum towards higher frequencies.¹⁴ This increases the bandwidth requirements of the tip-tilt compensation system significantly.

The contribution of this publication is the design and implementation of a closed-loop tip-tilt compensation system for the increased bandwidth requirements of tracking LEO objects. The proposed approach is a feedback control loop based on a custom made QPD as high-bandwidth tip-tilt sensor and FSM as compensating element. An optical breadboard carrying the proposed system is developed and attached to a small telescope to demonstrate the potential of the proposed system in on-sky experiments using a LEO object.

Further author information: (Send correspondence to Andreas Sinn)

Andreas Sinn.: E-mail: sinn@acin.tuwien.ac.at, Telephone: +43 1 58801 376525

2. TIP-TILT COMPENSATION SYSTEM IMPLEMENTATION

The proposed tip-tilt compensation system is developed on an optical breadboard and its block diagram is shown in Figure 1. The light collected by the telescope is collimated by lens L_{col} to a beam diameter of 12 mm. This lens may be repositioned along the optical axis to adjust the focal point of the compensation system to coincide with the one of the telescope. The compensating actuator is a FSM (OIM101, Optics in Motion LLC, CA, USA) driven by voice coils with a mechanical range of $\pm 1.5^\circ$ and a small-signal closed-loop bandwidth up to 800 Hz.²² A beam-splitter directs the beam to a camera (ASI 385 MC Cool, ZWO Company, China) and a custom-made QPD. The camera is used to record verification videos and observe both spot size and quality.

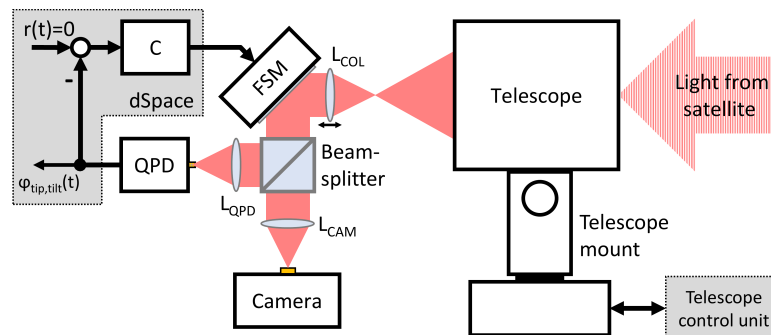


Figure 1. Block diagram of the used tip-tilt compensation system. The collected light is directed onto the FSM and then split into two paths, one for the QPD and one for the camera. The FSM is controlled based on the QPD output.

The QPD electronics are designed for high-sensitivity and are equipped with a low-pass filter with a bandwidth of 10 kHz. For the measurements presented in this publications the avalanche QPD QA4000-9 (First Sensor AG, Germany) with a wavelength sensitivity maximum at 905 nm is used. The position output signals of the QPD are normalized by the corresponding sum signal resulting in the error signals for tip $\varphi_{tip}(t)$ and tilt $\varphi_{tilt}(t)$, which are independent of the intensity of the incident light.²³ Signal acquisition and feedback control is implemented on a dSpace MicroLabBox (dSpace GmbH, Paderborn, Germany) running at a sampling frequency of 30 kHz. Custom made analog current controllers based on OPA549 (Texas Instruments, USA) drive the FSM.

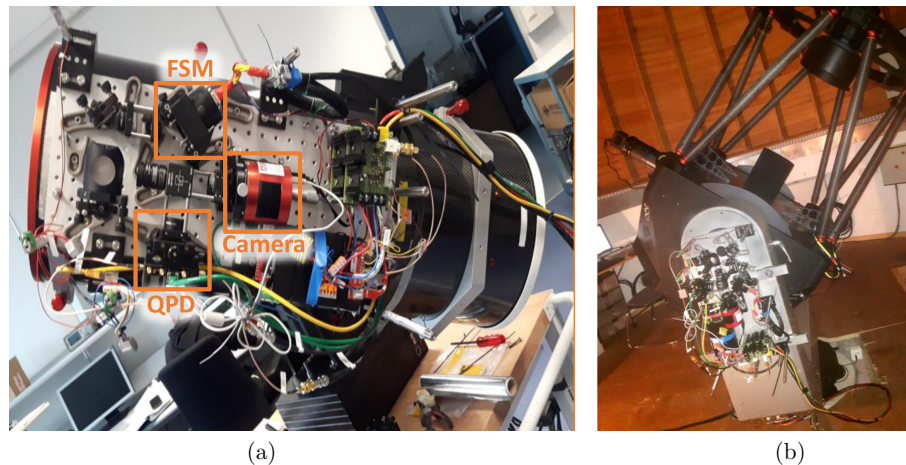


Figure 2. Proposed system for tip-tilt compensation mounted on an optical breadboard. (a) Mounted on 30 cm ASA Astrograph with highlighted components. (b) Mounted to a 80-cm ASA AZ800 telescope, which is used in this publication.

The developed compensation system may be mounted to different telescopes, as shown in Figure 2, using simple mechanical adapters. The measurements are conducted with a 80-cm AZ800 telescope system (ASA Astro Systeme GmbH, Neumarkt, Austria) with a focal ratio of 6.85. It is located on the countryside in Sandl, Austria at an altitude of 900 m. The telescope is equipped with a direct drive precision telescope mount designed for astronomy and LEO object tracking applications¹⁶ and set up in alt-az configuration. Stars and sunlight reflected by LEO objects are used as targets, offering a large variety of tracking velocities and elevations. The telescope mount is controlled by the *AStroAutoguide* software run by the telescope control unit (TCU).

3. BANDWIDTH REQUIREMENTS AND FEEDBACK CONTROL

To estimate the bandwidth requirements of a tip-tilt compensation system for LEO tracking applications the temporal properties of the tip $\varphi_{tip}(t)$ and tilt $\varphi_{tilt}(t)$ errors of a typical LEO object (COSMOS2315) are shown in Figure 3 in form of power spectral densities (PSDs). They are acquired using the system described in Section 2. The PSDs start with a $-\frac{2}{3}$ slope and converge to a $-\frac{11}{3}$ slope for high frequencies, which agrees with the analysis proposed by Tyler.²⁴ The corner frequency is approximately at 40 Hz, which is higher than usually experienced in astronomical applications.^{13,24} This is caused by fast slewing of the field of view of the telescope when tracking a LEO object, resulting in an increased velocity relative to the atmosphere.¹⁴ As frequency components up to 120 Hz with a significant contribution to the RMS error are visible in the PSDs, a requirement towards the closed-loop control bandwidth of a tip-tilt compensation system may be derived as follows: For a single actuator PID-controlled system the disturbance rejection increases by 20 dB per decade below the closed-loop bandwidth. Therefore, this bandwidth is typically set 5 to 10 times higher than the maximum frequency of the disturbance which shall be suppressed, which provides a disturbance rejection of at least a factor 5 for this frequency component. For the presented measurements this approach results in a minimum closed-loop bandwidth of 600 Hz.

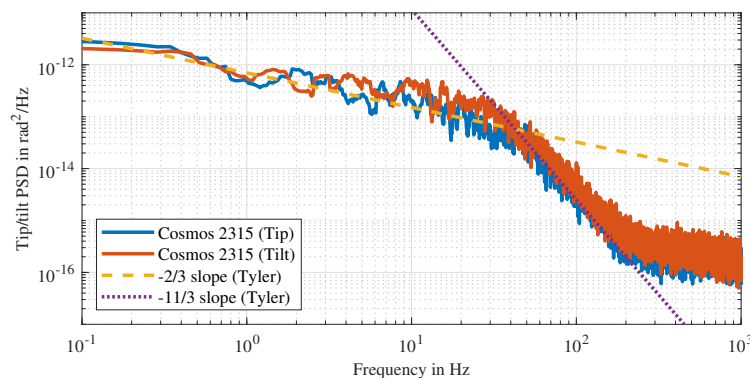


Figure 3. Power spectral densities of tip $\varphi_{tip}(t)$ and tilt $\varphi_{tilt}(t)$ without compensation measured at LEO object COSMOS2315. Two slopes as proposed by Tyler²⁴ are fitted to the tip signal.

To design a suitable controller the system dynamics have to be taken into account. The used FSM may be modeled as second order system²⁵ and is the only component of the proposed system with a significant dynamic behavior in the frequency range of interest, given by its suspension mode at 27 Hz.²⁶ The used QPD shows a first order low-pass characteristic with a cut-off frequency of 10 kHz. A typical approach to control a second order system such as this voice coil actuated FSM is proportional-integral-derivative (PID) control.²³ As the cross-talk between tip and tilt axes is small (20 dB below the system dynamics, data not shown) a SISO approach implementing two independent controllers, one for each axis, is justified. Therefore, two SISO-PID controllers are designed for the tip and tilt axes with focus on disturbance rejection and resulting in a bandwidth of 630 Hz with a phase margin of 60° and a gain margin of 20 dB.

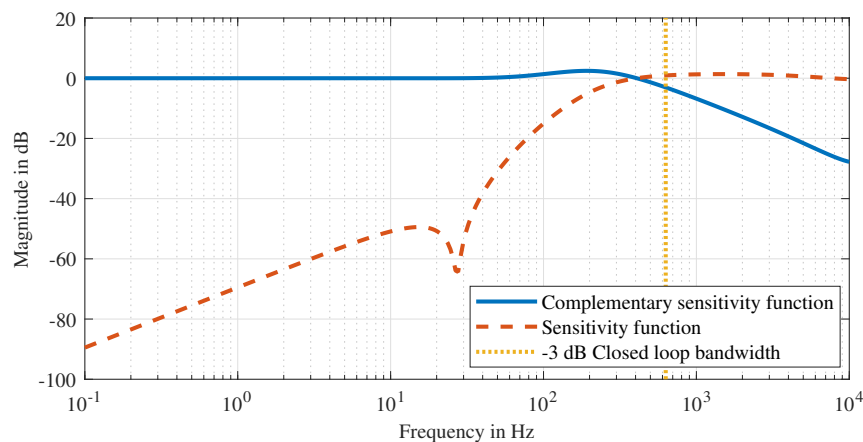


Figure 4. Simulated frequency behavior of the closed loop tip axis. Complementary sensitivity (solid blue) indicating a closed-loop bandwidth of 630 Hz and sensitivity function (dashed orange) quantifying the achievable disturbance rejection. The tilt axis shows similar behavior.

The simulated dynamic behavior of the resulting closed loop system of the tip axis is shown in Figure 4. The tilt axis shows comparable results. The complementary sensitivity (solid blue) function characterizes how well the system follows a reference input and also indicates the closed-loop bandwidth of the system. As intended the system shows constant reference tracking behavior until this bandwidth. The sensitivity function (dashed orange) is a measure of the ability of the system to reject disturbances. Due to the -20 dB per decade roll-on it is evident, that higher closed-loop bandwidths lead to a increased disturbance rejection at lower frequencies. Furthermore, it can be seen that the suspension mode of the FSM is turned into a notch in the sensitivity function, significantly increasing the disturbance rejection around this frequency. A rejection of 14 dB at 120 Hz is possible which equals approximately a factor 4.5 in reduction of an output error at this frequency.

4. MEASUREMENT RESULTS AND DISCUSSION

To evaluate the performance of the developed tip-tilt compensation system the results of a measurement series conducted in January 2020 are presented in this section.

Figure 5 presents the measured tip-tilt error signals for LEO object COSMOS2315 with an average orbit height approx. 1000 km. The weather conditions were clear but windy with a temperature at the observatory of -2 °C. Information on the orbit is given by the two subplots on the right side, which depict the elevation and total velocity (both dotted) of the tracked object as well as the duration of recording highlighted in green. A maximum velocity of 1.2 dps is reached at the end of this sample. The recorded time signals - tip $\varphi_{tip}(t)$ and tilt $\varphi_{tilt}(t)$ errors - are shown on the left side. For the first 10 seconds no compensation is active and the recorded deviations are the result of atmospheric turbulence, tracking uncertainties and vibrations. The mean value of both tip and tilt signals is removed to allow a direct comparison of off- and on-phases. After 10 seconds the tip-tilt compensation is enabled and the resulting error signals are recorded. A closed-loop compensation bandwidth of 630 Hz is used as described in Section 3. Transients after enabling the compensation are not shown, as their duration is short and the signal of interest is the residual error. A clear reduction of the RMS tip-tilt errors by up to a factor of 5 is visible in both axes.

To demonstrate the effect of tip-tilt compensation on an imaging system the integrated camera of the optical bench is used to record a series of images of the target object. The data from the same pass as shown in Figure 5 is used. All images of a sample of 10 s are stacked on top of each other to create a long-term exposure image. Figure 6(a) shows the resulting image without compensation, while Figure 6(b) presents the result with active tip-tilt compensation. For this comparison the offset (mean value of the distance from image center) of the uncompensated sample has not been removed. Generally, the object may be well within the field of view of the

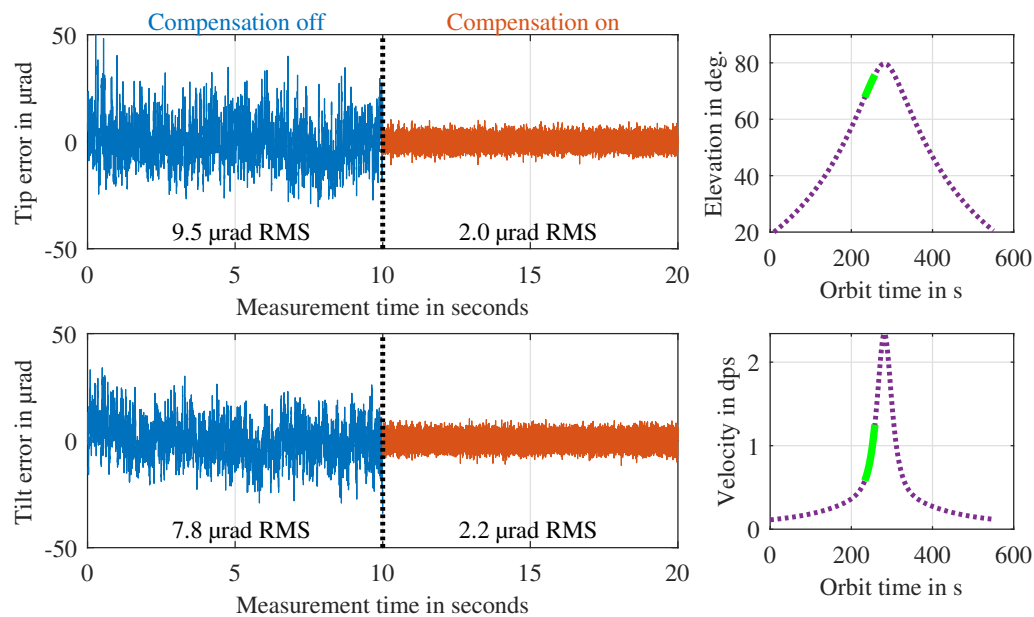


Figure 5. Measured tip-tilt error time signals $\varphi_{tip}(t)$ and $\varphi_{tilt}(t)$ (left) acquired from LEO object COSMOS2315 with an ASA AZ800 telescope without and with active compensation. At second 10 feedback control is enabled reducing the residual error significantly. On the right side the corresponding elevation and total velocity of the object's pass are shown with the record duration highlighted in green.

system during open loop tracking of a high-precision telescope mount and remains approximately constant over a full pass of the object. However, even a small offset from the image center (which coincides with the optical axis of the optical bench) may contribute significantly to a degradation of the performance. The Full-Width-Half-Maximum (FWHM) is reduced from $45 \times 43 \mu\text{rad}$ without to $18 \times 13 \mu\text{rad}$ with tip-tilt compensation. This is one important step towards a diffraction limited system and in terms of FSO communication enables higher performance as the received light is concentrated in a smaller area, thus enabling a smaller detector size.

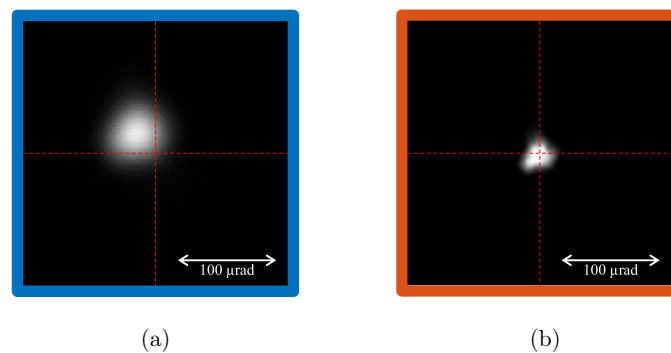


Figure 6. Long-term exposure images without (a) and with tip-tilt (b) compensation of object COSMOS2315.

The presented results confirm the performance of the proposed tip-tilt compensation system for LEO object tracking applications achieving a reduction of the RMS tip-tilt errors by up to a factor of 5. The residual error

remains constant around 2 μrad RMS for satellite speeds up to 1.2 dps, which is considered sufficient for the target applications.

5. CONCLUSION

In this publication, a high-bandwidth tip-tilt compensation system is presented as an effective option for small telescope systems and evaluated in on-sky experiments using low-Earth-orbit (LEO) objects. The compensation system utilizes feedback control based on the measurements of a quad-photo-diode (QPD) and a fast-steering mirror (FSM) as compensating actuator. Due to an increased disturbance bandwidth when tracking objects with velocities up to several degrees per second, a higher compensation bandwidth than in traditional astronomical applications is required. Furthermore, a higher compensation bandwidth enables increased disturbance rejection for all applications, thus enabling the full performance of small telescope systems.

Experimental campaigns are conducted at an observatory on the countryside in Austria. Exemplary measurement results acquired from reflected sunlight of the LEO object COSMOS 2315 are presented, showing that the developed the tip-tilt compensation system effectively reduces the RMS tip-tilt error by a factor of up to 5. The presented results successfully demonstrate the potential of tip-tilt compensation for small telescope systems especially for applications such as FSO satellite communication and space debris imaging.

ACKNOWLEDGMENTS

The authors gratefully acknowledge the excellent cooperation with ASA Astrosysteme GmbH and thank for their support and fruitful discussions.

This work has been by the Austrian Ministry for Transport, Innovation and Technology (BMVIT) under the scope of the Austrian Space Applications Program (FFG project number 854050) and is funded by the Austrian defense research programme FORTE of the Federal Ministry of Agriculture, Regions and Tourism (BMLRT).

REFERENCES

- [1] Ringwald, F., Culver, J., Lovell, R., Kays, S., and Torres, Y., “The Research Productivity of Small Telescopes and Space Telescopes,” *arXiv: Astrophysics* (astro-ph/0309772) (2003).
- [2] Chun, F. K., Tippetts, R. D., Strong, D. M., Della-Rose, D. J., Polsgrove, D. E., et al., “A new global array of optical telescopes: The falcon telescope network,” *Publications of the Astronomical Society of the Pacific* **130**(991) (2018).
- [3] Gebhardt, P., Schrimpf, A., Dersch, C., Spasovic, M., Bringmann, L., et al., “U-SMART: Small aperture robotic telescopes for universities,” *Revista Mexicana de Astronomia y Astrofisica: Serie de Conferencias* **51**, 44–46 (2017).
- [4] Šilha, J., “Small telescopes and their application in space debris research and space surveillance tracking,” *Contributions of the Astronomical Observatory Skalnaté Pleso* **49**(2), 307–319 (2019).
- [5] Ploner, M., Keller, P., Bibl, M., Döberl, E., Promper, W., and Weininger, D., “Ultrafast Wide Field Telescope for Space Debris Detection and Tracking,” *Proceedings of the Advanced Maui Optical and Space Surveillance Technologies Conference* (2019).
- [6] Steindorfer, M. A., Kirchner, G., Koidl, F., Wang, P., Jilete, B., and Flohrer, T., “Daylight space debris laser ranging,” *Nature Communications* **11**(1), 2–5 (2020).
- [7] Wang, P., Steindorfer, M. A., Koidl, F., Kirchner, G., and Leitgeb, E., “Megahertz repetition rate satellite laser ranging demonstration at Graz observatory,” *Optics Letters* **46**, 937–940 (2021).
- [8] McGarry, J. F., Hoffman, E. D., Degnan, J. J., Cheek, J. W., Clarke, C. B., et al., “NASA’s Satellite Laser Ranging Systems for the 21st Century,” *Journal of Geodesy* **93**, 2249–2262 (2019).
- [9] Liao, S. K., Cai, W. Q., Handsteiner, J., Liu, B., Yin, J., et al., “Satellite-relayed intercontinental quantum network,” *Phys. Rev. Lett* **120**(030501) (2018).
- [10] Fuchs, C., Brechtelsbauer, M., Schmidt, C., Akioka, M., Munemasa, Y., et al., “SOTA optical downlinks to DLR’s optical ground stations,” in *[ICSO 2016]*, **10562**, 1228 – 1236 (2017).

- [11] Riesing, K., Yoon, H. and Cahoy, K., "A portable optical ground station for low-earth orbit satellite communications," in [*Proc. of IEEE International Conference on Space Optical Systems and Applications*], 118–124 (2017).
- [12] National Aeronautics and Space Administration, "NASA Technology Taxonomy 2020," (2020).
- [13] Hardy, J. W., [*Adaptive optics for astronomical telescopes*], Oxford University Press, New York (1998).
- [14] Andrews, L. C. and Phillips, R. L., [*Laser beam propagation through random media: Second edition*], SPIE (2005).
- [15] Tyson, R., [*Principles of Adaptive Optics*], CRC Press, third ed. (2010).
- [16] Riel, T., Galfy, A., Janisch, G., Wertjan, D., Sinn, A., et al., "High performance motion control for optical satellite tracking systems," *Advances in Space Research* **65**(5) (2020).
- [17] Watson, J., "Tip-Tilt Correction for Astronomical Telescopes using Adaptive Control," in [*Wescon – Integrated Circuit Expo*], (1997).
- [18] Dekany, R., Brack, G., Palmer, D. and Oppenheimer, B. R., "First tip/tilt correction with the Palomar 200" adaptive optics system," in [*Conference on Adaptive Optical System Technologies*], 56–59, SPIE (1998).
- [19] Wizinowich, P., Adkins, S., Dekany, R., Gavel, D., Max, C., et al., "W. M. Keck Observatory's Next Generation Adaptive Optics Facility," *SPIE Proceedings* **7736**, 1–21 (2010).
- [20] Glindemann, A., Hippler, S., Berkefeld, T. and Hackenberg, W., "Adaptive optics on large telescopes," *Experimental Astronomy* **10**(1), 5–47 (2000).
- [21] Tyson, R. K. and Canning, D. E., "Indirect measurement of a laser communications bit-error-rate reduction with low-order adaptive optics," *Applied Optics* **42**(21), 4239 – 4243 (2003).
- [22] Csencsics, E. and Schitter, G., "Parametric PID controller tuning for a fast steering mirror," in [*1st Annual IEEE Conference on Control Technology and Applications*], 1673–1678 (2017).
- [23] Munning Schmidt, R., Schitter, G., Rankers, A. and Van Eijk, J., [*The Design of High Performance Mechatronics*], Delft University Press, 3rd ed. (2020).
- [24] Tyler, G. a., "Bandwidth considerations for tracking through turbulence," *Journal of the Optical Society of America A* **11**(1), 358 (1994).
- [25] Csencsics, E. and Schitter, G., "System Design and Control of a Resonant Fast Steering Mirror for Lissajous-Based Scanning," *IEEE/ASME Transactions on Mechatronics* **22**(5), 1963–1972 (2017).
- [26] Sinn, A., Riel, T., Deisl, F., Schachner, S., and Schitter, G., "High-bandwidth tip-tilt vibration compensation in telescope systems," in [*Proceedings of the Joint Conference 8th IFAC Symposium on Mechatronic Systems (Mechatronics 2019)*], 549–554 (2019).